Kobe University Repository : Kernel

PDF issue: 2025-12-04

Fourth-order Raman spectroscopy of adsorbed organic species on TiO2 surface

Nomoto, Tomonori
Onishi, Hiroshi

(Citation)
Chemical Physics Letters,455(4-6):343-347

(Issue Date)
2008-04-10

(Resource Type)
journal article

(Version)
Accepted Manuscript

(URL)
https://hdl.handle.net/20.500.14094/90000949

Fourth-order Raman spectroscopy of adsorbed organic species on TiO_2 surface

Tomonori Nomoto and Hiroshi Onishi*

Department of Chemistry, Faculty of Science, Kobe University, Nada, Kobe, 657-8501, Japan

Core Research for Evolutional Science and Technology, Japan Science and Technology Agency, Honmachi, Kawaguchi, 332-0012, Japan

*Corresponding author: nomoto@kobe-u.ac.jp. Fax number: +81-78-803-5674.

Abstract

We present the fourth-order Raman spectrum of an organic adsorbate on a solid surface. TiO_2 (110) surfaces covered by *p*-nitrobenzoate (*p*NB) and trimethyl acetate were observed. In addition to phonon modes of TiO_2, a weak band at 572 cm^{-1} was observed for the surface covered by *p*NB, and assigned as a molecular vibration. The coverage of *p*NB was estimated to be 13% using XPS. The feasibility of fourth-order Raman spectroscopy is demonstrated in observing organic adsorbates of submonolayer quantity.

Introduction

Molecules at interfaces play important roles in various chemical reactions. For determination of the molecular structures at the interfaces, various spectroscopic and microscopic methods have been developed. Molecular vibrations have been one of the most informative properties for identification of molecules and their structural changes in chemical reactions. Since even-order non-linear optical processes have come to be allowed only on interfaces for centro-symmetric media, sum frequency (SF) generation has been an interface-selective method to observe molecular vibrations [1-11]. For measurement of SF spectroscopy, infrared (IR) and visible (VIS) lights are mixed to generate the signal light. However, applicable interfaces are usually limited to media with small IR absorption. For that reason, interface-selective vibrational spectroscopy without IR light is a preferred method. Fourth-order Raman (FR) spectroscopy has recently been developed as interface-selective vibrational spectroscopy using only UV-VIS light [11-21]. FR spectroscopy has been applied to several interfaces including vacuum-solid [11-13,16], air-solid [17], solid-solid [14], air-liquid [15,18,19], liquid-liquid [20], and liquid-solid interfaces [21]. In FR spectroscopy, vibrational coherence generated by stimulated Raman process is probed by second-harmonic generation of probe pulses. Using time domain measurements of FR spectroscopy with 20 fs pulses, low frequency vibrations below 800 cm^{-1} are observable. The FR spectroscopy is therefore a promising method for characterizing interfaces buried in IR adsorbing media, especially in water.

However, there has been no reported FR spectrum of adsorbed molecules on

solid surfaces. Recently, we have reported FR spectra of TiO_2 rutile (110) surface covered with trimethyl acetate ($C(CH_3)_3COO^-$, hereafter abbreviated as TMA). In the spectra, several vibrational modes were observed, and we have assigned the observed bands as phonon modes of TiO_2 near the surface because there were corresponding bulk or surface phonon modes of TiO_2. On the other hand, no molecular vibration of TMA was observed in the spectra because TMA has no resonance to fundamental and second harmonic wavelength of pump and probe pulses (630 nm and its second harmonic at 315 nm). In the present study, we measured a TiO_2 (110) surface covered with *p*-nitrobenzoate (NO_2-C_6H_4-COO^-, *p*NB) and first observed molecular vibrations of adsorbates. We chose *p*NB as adsorbate because it is substitutable carboxylate from TMA, and two-photon resonance is expected because *p*NB has absorption around 300 nm. Second harmonic generation from adsorbed *p*-nitrobenzoic acid on silica was also reported [22]. We have demonstrated that TMA anions adsorbed on TiO_2(110) are exchanged with another carboxylate: retinoate [10], fluorescein isomer [23], and a ruthenium complex [24]. *p*BN, a carboxylate smaller than the three, can also be assumed to exchange TMA anions on TiO_2(110).

Experimental

TMA covered TiO_2 (110) crystals were prepared in an ultra-high vacuum (UHV) chamber. A one-side polished TiO_2 (110) crystal ($10 \times 10 \times 0.5$ mm^3, by Shinkosha, Co. Ltd., Japan) was Ar-ion sputtered at room temperature and annealed at 1000 K in a vacuum of 2×10^{-9} Torr. The resulting TiO_2 (110) surface was slightly

reduced to blue in color and had a (1×1) pattern in low-energy electron diffraction. The TiO_2 (110)-(1×1) surface was then exposed in trimethyl acetic acid vapor of 1×10^{-5} Torr for 60 s at room temperature, and a (2×1)-ordered monolayer of TMA was prepared on the TiO_2 (110) surface. The resulting TMA covered TiO_2 (110) was removed from the vacuum. It is stable in the air [10, 17]. A rutile TiO_2 (110) surface covered with *p*NB was prepared by immersion of the TMA covered TiO_2 (110) crystal into 6 mmol/L *p*-nitrobenzoic acid solution of dichrolomethane for five days. *p*-nitrobenzoic acid was used as received from Tokyo Chemical Industry. HPLC grade dichloromethane was used as solvent which was purchased from Wako Pure Chemical Industries. The immersed TiO_2 crystal was removed from the solution and washed by dichrolomethane for six hours, and used for the experiment in the air. TMA is adsorbed on the TiO_2 (110) surface in a bridge-bonded fashion [10]. Benzoic acid also adsorbs to TiO_2 surface in a bridge-bonded fashion [25], hence *p*NB is also expected to be bridge-bonded on TiO_2 surface (Figure 1).

The experimental setup of the FR measurement is essentially the same as that in our previous reports [17]. In brief, pump and probe pulses were from a non-colinear optical parametric amplifier (Quantronix, TOPAS-*white*) pumped by a Ti:Sapphire regenerative amplifier (Spectra-Physics, Hurricane). The center wavelength of the pulses was tuned at 550 nm, and the pulse width was 25 fs as a result of cross correlation of pump and probe pulses on the sample surface. Pump and probe pulses were *p*-polarized and focused on the sample (8 mJ/cm^2 each). The second harmonic light generated from the probe pulse was detected by a photomultiplier. The incident

angle of the pump and probe pulses was 55 degrees from the surface normal, and the angle between the pump and probe pulses was 2 degrees. The time delay was scanned from -0.3 to 3 ps at 5 fs step. 161300 pulses were integrated to obtain the SH time profile at each time step for the *p*NB covered surface. 339125 pulses were integrated for TMA covered surface. The integration number was dependent on laser stability to obtain spectra with similar signal-to-noise (S/N) ratio. The irradiated position was moved on the crystal surface after each scan of the delay at approximately 1500 (*p*NB) and 2400 points (TMA). Two samples which were prepared in the same way were used for the TMA covered surface. In the case of the *p*NB covered surface, one sample was used.

For evaluation of the number of adsorbed *p*NB molecules, XPS measurements were performed using Al-Kα (1487 eV) with a detection angle of 45 degrees. Both a TMA covered surface and a *p*NB covered surface were measured. The samples were prepared separately from the FR measurement in the same preparation method. The spectrometer used was ULVAC-PHI Quantum-2000 at Ion Engineering Research Institute Corporation.

Results and Discussion

The obtained time profile of second harmonic intensity of probe pulses for the *p*NB covered TiO_2 surface is shown in Figure 2(a). $I(2\omega)/I_0(2\omega)$ is the pumped SH intensity relative to the non-pumped SH intensity. A sharp negative peak at time zero and a decay of second harmonic intensity were essentially the same as the reported time

profile of the TMA covered surface [17].

The electric field of observed second harmonic can be treated as summation of periodically modulated ($E_{mod}(2\omega,\ t_d)$) and non-modulated ($E_{non}(2\omega,\ t_d)$) components. Because the modulations are originated from vibrational coherences generated by the pump pulse, E_{mod} is expressed by the sum of periodic modulations as,

$$E_{mod}(2\omega,t_d) \propto \chi^{(4)}(t_d) \propto \sum_v A_v \exp(i(\omega_v t_d + \varphi_v))\exp(t_d/T_v) \quad (1)$$

where A_v, ω_v, φ_v, T_v and t_d are the amplitude, frequency, phase, dephasing time of each vibrational mode and time delay of the probe pulse. $\chi^{(4)}$ is fourth-order response of the interface. The intensity of observed second harmonic is

$$I(2\omega,t_d) \propto \left|E_{non}(2\omega,t_d) + E_{mod}(2\omega,t_d)\exp(i\varphi_{non})\right|^2 \quad (2)$$

where φ_{non} represents relative phase between $E_{mod}(2\omega,\ t_d)$ and $E_{non}(2\omega,\ t_d)$. When $|E_{non}(2\omega,\ t_d)| >> |E_{mod}(2\omega,\ t_d)|$, the oscillation amplitude becomes proportional to the heterodyne component, which is

$$E_{non}(2\omega,t_d)\cdot E_{mod}(2\omega,t_d)\cdot \exp(i\varphi_{non}) \propto \sum_v A_v \exp(i(\omega_v t_d + \varphi_v + \varphi_{non}))\exp(-t_d/T_v) \quad (3).$$

In the case of one-photon resonant dye solution interfaces for example, cosine-type modulations with $\varphi_v + \varphi_{non} = 0°$ are reported [15, 20].

For obtaining the modulated component of the FR signal, non-modulated SH decay was fitted and subtracted by a mixed function composed of a Gaussian function, two Gaussian convoluted exponential functions, and a Gaussian convoluted step function for a component with decay constant over 100 ps. The mixed function reproduced the whole non-modulated SH time profile well. The obtained time constants of the decay were 130 fs, 1.6 ps, and the full width at half maximum (fwhm) of the

Gaussian function at the zero position was 32 fs. The modulated component which remained after subtraction is shown in Figure 2(b). To obtain the Fourier-transformed (FT) spectrum with a better S/N ratio, zero data was added to the end of the modulated component to 30 ps, and a Gaussian window function with 1 ps half width at half maximum was multiplied to the data before Fourier transformation. Multiplying the window function corresponds to a convolution of the FT spectrum with a Gaussian function having a fwhm of 15 cm^{-1}. The resulting FT spectrum of the *p*NB covered surface is shown in Figure 2(c). The imaginary part represents sine components of the oscillation ($\varphi_v + \varphi_{non} = 90°$), and real part represents cosine components of the oscillation ($\varphi_v + \varphi_{non} = 0°$).

For obtaining the wavenumber and the phase of vibrational coherences, the spectrum was simulated using sum of Lorentzian functions, which is defined as

$$S_{FRS}(\omega) = \sum_v \frac{A_v}{(\omega - \omega_v) + i\Gamma_v} \exp(i\theta_v) \tag{4}$$

where A_v, ω_v, Γ_v and θ_v are amplitude, center wavenumber, band width and phase of each mode. The phase is defined as $\theta_v = \varphi_v + \varphi_{non} + 90°$ in eq. (1). Six Lorentzian functions were used to fit the spectrum of the *p*NB-adsorbed surface. Five are for substantial vibrations of 825, 572, 439, 363, 180cm^{-1}, while one at 113 cm^{-1} represents the residue of the fit. Zero phase ($\theta_v = 0$) was initially assumed to minimize the number of fitting parameters. Two bands (825 cm^{-1} and 180 cm^{-1}) were successfully fit with $\theta_v = 0$, whereas finite phases were necessary for the other three bands to reproduce the observed spectrum. The obtained fitting parameters are shown in Table 1(a), and the

simulated spectrum is in Figure 2(c). Uncertainty of the simulated phases is dominated by precision of the zero time delay. The phase uncertainty was estimated and shown in Table 1, on the basis of the time zero uncertainty, ±3.4 fs for *p*NB-adsorbed TiO_2 and ±1.7 fs for TMA-covered TiO_2.

The raw SH intensity obtained from the TMA covered TiO_2 surface is shown in Figure 3(a). The non-modulated component was fitted using decay constants of 130 fs and 1.5 ps and a Gaussian fwhm of 32 fs. The obtained time constants of the fitting function were almost the same values for both the TMA and *p*NB covered surfaces. Because the trapping time of photo-excited electrons has a similar value in particle TiO_2 [26-29], we consider that the time constant of 130 fs corresponds to the trapping time of conduction-band electrons. The reason of the SH decay with picosecond time constant (1.5 ps) is not definite. Trapping of photo-excited holes following transport to the surface provides one possibility. Energy dissipation from electronic temperature to lattice temperature, or thermal diffusion from the surface to the bulk is another possibility.

The modulated component of the SH intensity and the FT spectrum are shown in Figure 3(b) and 3(c). The FR spectrum of the TMA covered TiO_2 surface have a good S/N ratio. Four major peaks at 824, 440, 366 and 181 cm^{-1} were in good agreement with what was observed on a TMA covered surface using 630 nm pulses [17]. The obtained spectrum was fitted with Lorentzian functions. The four major bands of the *p*NB covered surface and TMA covered surface were fitted with identical parameters shown in Table 1. The error of θ_v in Table 1(2) was also obtained from standard error of zero

position (±1.7 fs). Since there are corresponding bulk, or surface phonon modes of TiO_2 [30-35], these modes were assigned to phonon modes of TiO_2 near the surface. Different phases, 0° for 825 cm^{-1} and 180 cm^{-1} and 36° for 363 cm^{-1} band, suggest different excitation mechanisms of the phonon modes. Spectral structures below 100 cm^{-1} were artifacts derived from residue of the fittings.

In addition to the previously reported TiO_2 phonon bands, a band was observed at 572 cm^{-1} for the *p*NB covered surface. There is no corresponding bulk phonon mode of TiO_2 in this wavenumber region [30-32], and there is also no reported surface phonon mode around 570 cm^{-1} by HREELS [33-35]. Hence 572 cm^{-1} band should have originated from adsorption of *p*NB on TiO_2.

According to a normal mode analysis of Raman and IR spectra of vapor *p*NB radical dianion, 550 cm^{-1} (b_2) and 509 cm^{-1} (a_1) skeletal modes are reported [36]. These modes are also observed at around 530 cm^{-1} in surface enhanced Raman scattering (SERS) spectra of *p*-nitrobenzoic acid adsorbed on metal surfaces [37-42]. Roth *et al.* [40] indicated that adsorbed *p*-nitrobenzoic acid on metal surface was coupled to 4,4'-azodibenzoate ($^-$OOC-Ph-N=N-Ph-COO$^-$) by Ar-ion laser irradiation. 4,4'-azodibenzoate also has a broad SERS band at around 550 cm^{-1} [42]. Hence even if the same reaction occurs on the TiO_2 surface, it is difficult to distinguish the molecule only by this band. Characteristic bands to distinguish *p*NB and 4,4'-azodibenzoate are in a higher wavenumber region than those found in our measurement. Both SERS spectra of *p*-nitrobenzoic acid and 4,4'-azodibenzoate have relatively strong bands at around 710 cm^{-1} and 860 cm^{-1} in addition to 550 cm^{-1} [40, 42]. The two bands, if any, can be

masked on our spectrum because of a TiO_2 phonon mode at 825 cm^{-1}. A fourth-order Raman transition contains a Raman transition and a hyper-Raman transition. The intensity of the fourth-order response is not necessarily proportional to the intensity of SERS response. Thus, observed mode at 572 cm^{-1} is most likely to be a molecular vibration derived from adsorbed *p*NB or 4,4'-azodibenzoate.

The SH light intensity was not enhanced by the presence of *p*NB. This suggests that the SH light is mainly generated at the TiO_2 surface. When the fourth-order band at 572 cm^{-1} is generated by adsorbed *p*NB, some enhancement by two-photon resonance should be present. When the 4,4'-azodibenzoate is responsible for the 572 cm^{-1} band, one-photon resonance may occur in the fourth-order transition. The absorption of the 4,4'-azodibenzoate is expected at around 500 nm on the basis of the absorption of azobenzen derivatives.

The XPS results for Ti(2p) and N(1s) are shown in Figure 4. A peak was additionally observed at 407 eV for *p*NB covered TiO_2 which was the reported peak position of N(1s) in *p*-nitrobenzoic acid [43]. This result indicates the existence of adsorbed *p*NB on the TiO_2 surface. The larger peak at 401 eV is probably originated from impurities of the substrates because they were observed on both surfaces. In order to estimate the quantity of *p*NB, peak areas of N(1s) and Ti($2p_{3/2}$) were compared. The intensity ratio of the Ti($2p_{3/2}$) and N(1s) peak areas was $I_{N1s}/I_{Ti2p_{3/2}} = 0.0033$. The ratio can be described as,

$$I_{N1s}/I_{Ti2p_{3/2}} = \frac{\sigma_{N1s} \cdot \theta_N}{\sigma_{Ti2p_{3/2}} \cdot \theta_{Ti} \cdot \lambda_{TiO_2} \cdot \cos\alpha / d_{TiO_2}} \quad (5)$$

where $\sigma_{Ti2p_{3/2}}$ = 5.22 and σ_{N1s} = 1.80 are photoelectron emission cross sections relative to C(1s), θ_N and θ_{Ti} are the atom density of each layer (θ_{Ti} = 10.4 nm^{-2}), λ_{TiO_2} is the electron inelastic mean free path of TiO_2 (λ_{TiO_2} = 1.6 nm at 1000 eV [44]), α = 45° is the detection angle, and d_{TiO_2} = 0.324 nm is the layer-by-layer spacing of TiO_2 (110). θ_N = 0.35 nm^{-2} was obtained as a result. Here we assumed no screening effect of the Ti signal by adsorbed molecules because of low molecular coverage. Because a *p*NB has one nitrogen atom, the resulting θ_N corresponds to the molecular number density of the TiO_2 (110) surface.

A TiO_2 (110) surface covered with the TMA monolayer has a (2×1) order. Because a *p*NB has one carboxyl group as well as TMA, we assumed a similar ordered (2×1) monolayer for *p*NB at full coverage (Figure 1). In the case of 100% of TMA being exchanged to *p*NB, molecular number density is 2.6 nm^{-2}. The estimated number of N atoms corresponds to 13% of TMA exchanged by *p*NB.

Conclusion

In this study, we have observed fourth-order Raman response of an organic adsorbate on the TiO_2 (110) surface. A band appeared at 572 cm^{-1} on a *p*NB covered surface, in addition to stronger phonon modes of TiO_2 at 825, 439, 363, and 180 cm^{-1}. The 572 cm^{-1} band was most likely the skeletal vibration of adsorbed *p*NB or 4,4'-azodibenzoate. This provides a first successful application to organic adsorbates. Possible application to a wide range of adsorbates is expected.

Acknowledgement

The authors acknowledge Dr. Satoru Fujiyoshi for his helpful suggestions.

References

(1) Y. R. Shen, The Priciple of Nonlinear Optics, J. Wiley, New York, 1984.

(2) Y. R. Shen, Nature 337 (1989) 519.

(3) K. B. Eisenthal, Chem. Rev. 96 (1996) 1343.

(4) P. B. Miranda, Y. R. Shen, J. Phys. Chem. B 103 (1999) 3292.

(5) L. F. Scatena, M. G. Brown, G. L. Richmond, Science 292 (2001) 908.

(6) S. Roke, J. Schins, M. Müller, M. Bonn, Phys. Rev. Lett. 90 (2003) 128101.

(7) J. Wang, M. Even, X. Chen, A. H. Schmaier, J. H. Waite, Z. J. Chen, Am. Chem. Soc. 125 (2003) 9914.

(8) T. Ishibashi, H. Onishi, Appl. Spectrosc. 56 (2002) 1298.

(9) T. Ishibashi, H. Onishi, Appl. Phys. Lett. 81 (2002) 1338.

(10) T. Ishibashi, H. Uetsuka, H. Onishi, J. Phys. Chem. B 108 (2004) 17166.

(11) Y. Matsumoto, K. Watanabe, Chem. Rev. 106 (2006) 4234.

(12) Y. M. Chang, L. Xu, H. W. K. Tom, Phys. Rev. Lett. 78 (1997) 4649.

(13) K. Watanabe, N. Takagi, Y. Matsumoto, Chem. Phys, Lett. 366 (2002) 606.

(14) Y. M. Chang, Appl. Phys. Lett. 82 (2003) 1782.

(15) S. Fujiyoshi, T. Ishibashi, H. Onishi, J. Phys. Chem. B 108 (2004) 10636.

(16) U. Bovensiepen, A. Melnikov, I. Radu, O. Krupin, K. Starke, M. Wolf, E. Matthias, Phys. Rev. B 69 (2004) 235417.

(17) S. Fujiyoshi, T. Ishibashi, H. Onishi, J. Phys. Chem. B 109 (2005) 8557.

(18) Y. Hirose, H. Yui, T. J. Sawada, Phys. Chem. B 109 (2005) 13063.

(19) S. Yamaguchi, T. Tahara, J. Phys. Chem. B 109 (2005) 24211.

(20) S. Fujiyoshi, T. Ishibashi, H. Onishi, J. Phys. Chem. B 110 (2006) 9571.

(21) T. Nomoto, H. Onishi, Phys. Chem. Chem. Phys. 9 (2007) 5515.

(22) T. F. Heinz, H. W. K. Tom, Y. R. Shen, Phys. Rev. A 28 (1983) 1883.

(23) C. Pang, T. Ishibashi, H. Onishi, Jpn. J. Appl. Phys. 44 (2005) 5438.

(24) A. Sasahara, C. Pang, H. Onishi, J. Phys. Chem. B 110 (2006) 4751.

(25) Q. Guo, I. Cocks, E. M. Williams, Surf. Sci. 393 (1997) 1.

(26) D. P. Colombo, K. A. Roussel, J. Saeh, D. E. Skinner, J. J. Cavaleri, R. M. Bowman, Chem. Phys. Lett. 232 (1995) 207.

(27) D. E. Skinner, D. P. Colombo, J. J. Cavaleri, R. M. Bowman, J. Phys. Chem. 99 (1995) 7853.

(28) X. Yang, N. Tamai, Phys. Chem. Chem. Phys. 3 (2001) 3393.

(29) K. Iwata, T. Takaya, H. Hamaguchi, A. Yamakata, T. A. Ishibashi, H. Onishi, H. Kuroda, J. Phys. Chem. B 108 (2004) 20233.

(30) D. M. Eagles, J. Phys. Chem. Solids 25 (1964) 1243.

(31) S. P. S. Porto, P. A. Fleury, T. C. Damen, Phys. Rev. 154 (1967) 522.

(32) C. Lee, P. Ghosez, X. Gonze, Phys. Rev. B 50 (1994) 13379.

(33) G. Rocker, J. A. Schaefer, Phys. Rev. B 30 (1984) 3704.

(34) P. A. Cox, R. G. Edgell, S. Eriksen, W. R. Flavell, J. Electron Spectrosc. Relat. Phenom. 39 (1986) 117.

(35) M. A. Henderson, Surf. Sci. 355 (1996) 151.

(36) E. E. Ernstbrunner, R. B. Girling, R. E. Hester, J. Chem. Soc. Faraday Trans. II 74 (1978) 1540.

(37) R. Dornhaus, R. E. Benner, R. K. Chang, I. Chabay, Surf. Sci. 101 (1980) 367.

(38) P. F. Liao, M. B. Stern, Opt. Lett. 7 (1982) 483.

(39) D. A. Weitz, S. Garoff, J. I. Gersten, A. J. Nitzan, Chem. Phys. 78 (1983) 5324.

(40) P. G. Roth, R. S. Venkatachalam, F. J. Boerio, J. Chem. Phys. 85 (1986) 1150.

(41) H. Bercegol, F. J. Boerio, Langmuir 10 (1994) 3684.

(42) R. S. Venkatachalam, F. J. Boerio, P. G. Roth, J. Raman Spectrosc. 19 (1988) 281.

(43) K. Ihm, T. H. Kang, J. H.Han, S. Moon, C. C. Hwang, K. J. Kim, H. N. Hwang, C. H. Jeon, H. D. Kim, B. Kim, C. Y. Park, J. Electron Spectrosc. Relat. Phenom. 144-147 (2005) 397.

(44) G. G. Fuentes, E. Elizalde, F. Yubero, J. M. Sanz, Surf. Interface Anal. 33 (2002) 230.

Figure 1. An expected structure of *p*-nitrobenzoate adsorbed on TiO_2 (110) surface. Open circles indicate oxygen and black circles indicate titanium positions of TiO_2.

Figure 2. (a) Intensity change of the reflected second harmonic light from TiO_2 (110) surface covered with *p*NB. (b) Modulated component which remained after subtraction of the fitting curve. (c) Broad gray line is the FT spectrum of FR response of TiO_2 (110) covered with *p*NB. Black broken line presents spectral simulation.

Figure 3. (a) Intensity change of the reflected second harmonic light from TiO_2 (110) surface covered with TMA. (b) Modulated component which remained after subtraction of fitting curve. (c) Broad gray line is the FT spectrum of FR response of TiO_2 (110) covered with TMA. Black broken line presents spectral simulation.

Figure 4. XPS results of TiO_2 (110) surface covered with *p*NB and TMA. (a)-(b): Ti_{2p} peaks of TiO_2 (110) surface covered with (a) *p*NB and (b) TMA. (c)-(d): N_{1s} peaks of TiO_2 (110) surface covered with (c) *p*NB and (d) TMA. Circle or cross markers indicate data points of XPS. Dotted lines indicate baselines used for subtraction in coverage calculation of *p*NB.

Table 1. Fitting parameters of FR spectra of TiO_2 (110) surface covered with (a) *p*NB and (b) TMA.

(a) *p*NB covered TiO_2

ω_v / cm^{-1}	Γ_v / cm^{-1}	A_v	θ_v / deg.	error of θ_v
825	37	5.8	0° (fixed)	30°
572	14	0.2	32°	21°
439	17	2.2	-23°	16°
363	11	0.8	-36°	13°
180	24	6.1	0° (fixed)	7°
baseline				
113	148	-15	-44°	

(b) TMA covered TiO_2

ω_v / cm^{-1}	Γ_v / cm^{-1}	A_v	θ_v / deg.	error of θ_v
824	31	2.4	0° (fixed)	15°
440	19	1.2	-24°	8°
366	10	0.5	-35°	7°
181	22	2.7	0° (fixed)	3°
baseline				
125	174	-7.5	-39°	

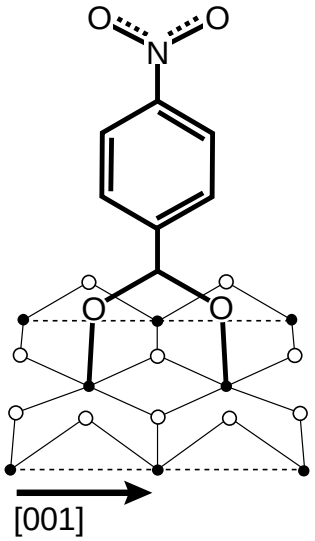

Figure 1.

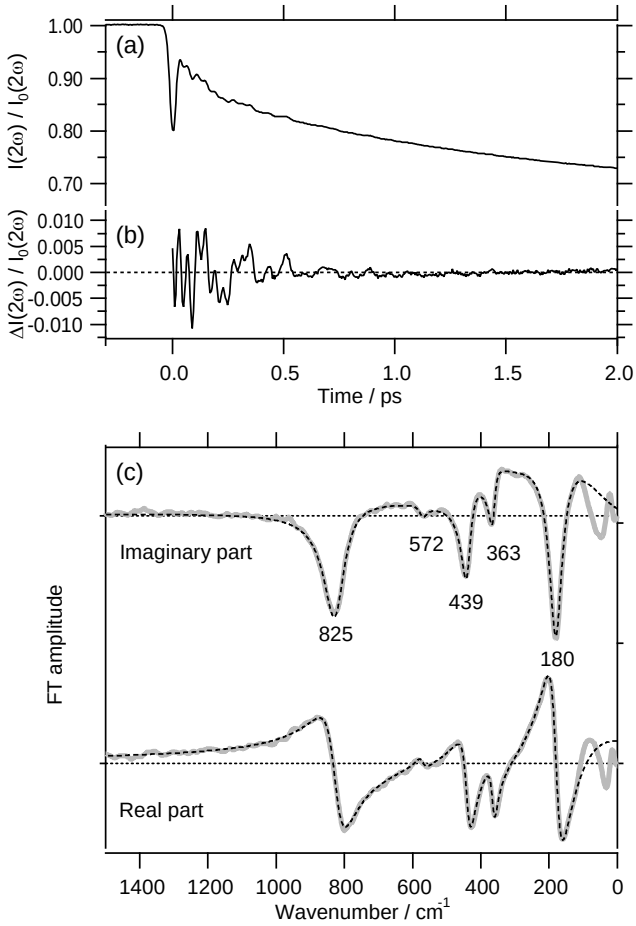
(a)
(b)
(c)
I(2ω) / I0(2ω)
ΔI(2ω) / I0(2ω)
1.00
0.90
0.80
0.70
0.010
0.005
0.000
-0.005
-0.010
0.0
0.5
1.0
1.5
2.0
Time / ps
Imaginary part
Real part
FT amplitude
825
572
439
363
180
1400
1200
1000
800
600
400
200
0
Wavenumber / cm-1

Figure 2.

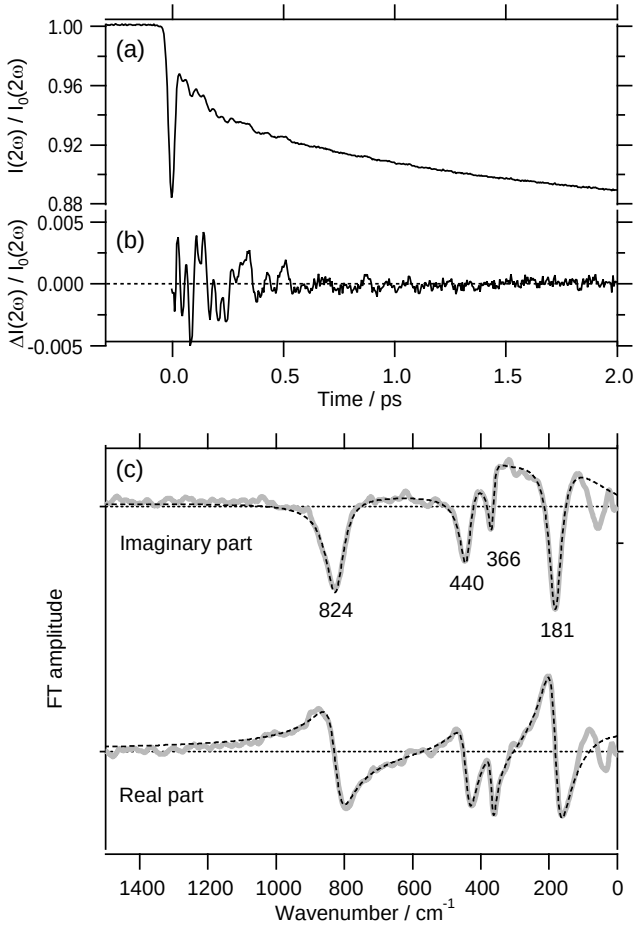
(a)
(b)
(c)
I(2ω) / I0(2ω)
ΔI(2ω) / I0(2ω)
1.00
0.96
0.92
0.88
0.005
0.000
-0.005
0.0
0.5
1.0
1.5
2.0
Time / ps
Imaginary part
Real part
824
440
366
181
FT amplitude
1400
1200
1000
800
600
400
200
0
Wavenumber / cm-1

Figure 3.

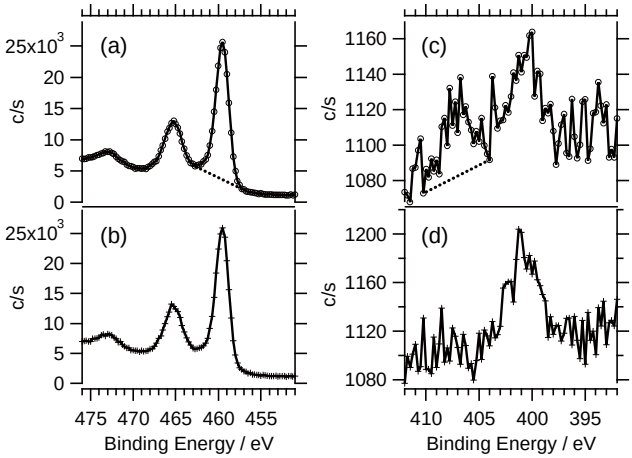
(a)
(b)
(c)
(d)
25x10^3
20
15
10
5
0
c/s
1160
1140
1120
1100
1080
1200
1160
1120
1080
475 470 465 460 455
Binding Energy / eV
410 405 400 395
Binding Energy / eV

Figure 4.